

A structural, magnetic and Mössbauer spectral study of the magnetocaloric  
 $\text{Mn}_{1.1}\text{Fe}_{0.9}\text{P}_{1-x}\text{Ge}_x$  compounds

This article has been downloaded from IOPscience. Please scroll down to see the full text article.

2008 J. Phys.: Condens. Matter 20 475206

(<http://iopscience.iop.org/0953-8984/20/47/475206>)

View [the table of contents for this issue](#), or go to the [journal homepage](#) for more

Download details:

IP Address: 129.252.86.83

The article was downloaded on 29/05/2010 at 16:39

Please note that [terms and conditions apply](#).

# A structural, magnetic and Mössbauer spectral study of the magnetocaloric $\text{Mn}_{1.1}\text{Fe}_{0.9}\text{P}_{1-x}\text{Ge}_x$ compounds

Moulay T Sougrati<sup>1</sup>, Raphaël P Hermann<sup>1,2</sup>, Fernande Grandjean<sup>1</sup>, Gary J Long<sup>3</sup>, E Brück<sup>4</sup>, O Tegus<sup>4</sup>, N T Trung<sup>4</sup> and K H J Buschow<sup>4</sup>

<sup>1</sup> Department of Physics, B5, University of Liège, B-4000 Sart-Tilman, Belgium

<sup>2</sup> Institut für Festkörperforschung, Forschungszentrum Jülich GmbH, D-52425 Jülich, Germany

<sup>3</sup> Department of Chemistry, Missouri University of Science and Technology, Rolla, MO 65409-0010, USA

<sup>4</sup> Van der Waals-Zeeman Instituut, Universiteit van Amsterdam, Valckenierstraat 65, NL-1018XE Amsterdam, The Netherlands

E-mail: [fgrandjean@ulg.ac.be](mailto:fgrandjean@ulg.ac.be) and [glong@mst.edu](mailto:glong@mst.edu)

Received 23 August 2008, in final form 9 October 2008

Published 29 October 2008

Online at [stacks.iop.org/JPhysCM/20/475206](http://stacks.iop.org/JPhysCM/20/475206)

## Abstract

The structural, magnetic and Mössbauer spectral properties of the magnetocaloric  $\text{Mn}_{1.1}\text{Fe}_{0.9}\text{P}_{1-x}\text{Ge}_x$  compounds, with  $0.19 < x < 0.26$ , have been measured between 4.2 and 295 K. The 295 K unit-cell volume increases from  $x = 0.19$  to 0.22 and is substantially smaller in the ferromagnetic  $\text{Mn}_{1.1}\text{Fe}_{0.9}\text{P}_{0.74}\text{Ge}_{0.26}$ . The temperature dependence of the magnetization reveals a ferromagnetic to paramagnetic transition with a Curie temperature between approximately 250 and 330 K and hysteresis width of 10 to 4 K, for  $0.19 < x < 0.25$ . The composition  $\text{Mn}_{1.1}\text{Fe}_{0.9}\text{P}_{0.78}\text{Ge}_{0.22}$  shows the largest isothermal entropy change of approximately 10 J/(kgKT) at 290 K. The Mössbauer spectra have been analysed with a binomial distribution of hyperfine fields correlated with a change in isomer shift and quadrupole shift, a distribution that results from the distribution of phosphorus and germanium among the near neighbours of the iron. The coexistence of paramagnetic and magnetically ordered phases in ranges of temperature of up to 50 K around the Curie temperature is observed in the Mössbauer spectra and is associated with the first-order character of the ferromagnetic to paramagnetic transition. The temperature dependence of the weighted average hyperfine field is well fitted within the magnetostrictive model of Bean and Rodbell. Good fits of the Mössbauer spectra could only be achieved by introducing a difference between the isomer shifts in the paramagnetic and ferromagnetic phases, a difference that is related to the magnetostriction and electronic structure change.

(Some figures in this article are in colour only in the electronic version)

## 1. Introduction

In the twenty-first century, refrigeration is still conventionally carried out through vapour-compression technology in everyday applications. However, environmental concern is growing and environmentally friendly cooling techniques, such as thermoelectric cooling [1] and magnetic refrigeration [2], are more often considered as viable alternative techniques because they are becoming increasingly efficient and

affordable. Improvements in efficiency and affordability are based on the synthesis and design of new materials with improved physical properties, materials that can be produced at low cost. These goals can only be reached through detailed studies of the fundamental physical properties associated with the thermoelectric cooling and magnetocaloric refrigeration power.

During the second half of the twentieth century the search for magnetocaloric compounds [3] has evolved from

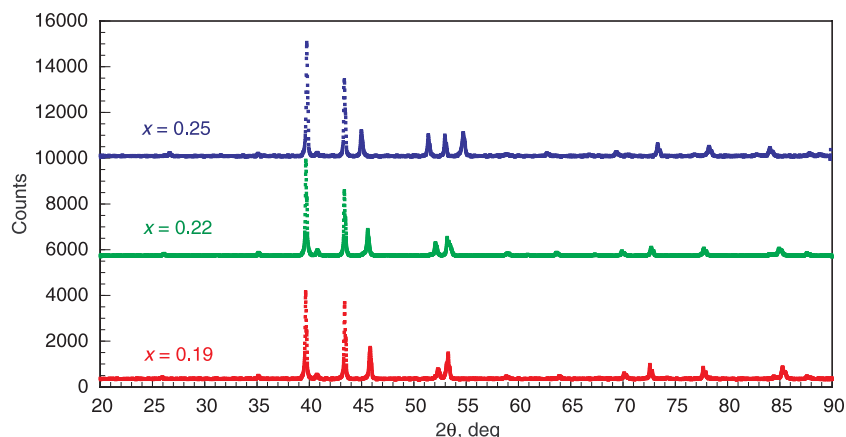


**Figure 1.** The 295 K x-ray powder diffraction patterns of the  $\text{Mn}_{1.1}\text{Fe}_{0.9}\text{P}_{1-x}\text{Ge}_x$  compounds, with  $x = 0.19, 0.22$  and  $0.25$ .

rare-earth-based compounds, compounds that exhibit large magnetic moments but are expensive, to transition-metal-based intermetallic compounds, compounds that exhibit smaller magnetic moments but are far less expensive. Because among the transition metals, manganese may exhibit a magnetic moment as large as  $4 \mu_B$ , research efforts have concentrated on manganese-containing compounds. The recent discovery [4] of a giant magnetocaloric effect in the  $\text{MnFeP}_{1-x}\text{As}_x$  compounds has initiated intense research activity [3, 5–12] on the  $\text{Fe}_2\text{P}$ -type family of compounds.

Because of the presence of toxic, and thus undesirable, arsenic in the  $\text{MnFeP}_{1-x}\text{As}_x$  compounds, the replacement of arsenic by silicon [8] or germanium [7, 9–13] and its effect on the magnetocaloric properties have been investigated. The series of  $\text{MnFeP}_{1-x}\text{Ge}_x$  compounds, with  $x$  between 0.2 and 0.3, has been found [7] to be ferromagnetic with Curie temperatures increasing from 250 to 380 K and to have a magnetocaloric effect similar to that observed [4] in the  $\text{MnFeP}_{1-x}\text{As}_x$  compounds.

In view of these interesting magnetocaloric properties near room temperature, a detailed investigation of the  $\text{MnFeP}_{1-x}\text{Ge}_x$  compounds is important. Because the iron-57 Mössbauer spectral study [5] of the  $\text{MnFeP}_{1-x}\text{As}_x$  compounds has been very informative, the  $\text{Mn}_{1.1}\text{Fe}_{0.9}\text{P}_{1-x}\text{Ge}_x$  compounds, with  $x = 0.16, 0.20, 0.22$  and  $0.26$ , have been studied herein by iron-57 Mössbauer spectroscopy combined with x-ray diffraction and magnetic measurements.

## 2. Experimental details

Polycrystalline samples of the  $\text{Mn}_{1.1}\text{Fe}_{0.9}\text{P}_{1-x}\text{Ge}_x$  compounds, with  $x = 0.16, 0.20, 0.22$  and  $0.26$ , were prepared by high-energy ball milling and solid state reaction from 99.5% pure  $\text{Fe}_2\text{P}$ , obtained from Alfa Aesar, 99.9% pure manganese chips, 99.99% pure red phosphorus powder and 99.999% pure germanium [7]. The ball milled powder was heated in a molybdenum crucible in a 100 mbar argon atmosphere at 1273 K for 5 h followed by annealing at 873 K for 50 h. The powder x-ray diffraction patterns were obtained with a Philips X'pert diffractometer equipped with  $\text{Cu K}\alpha$  radiation.

The magnetic measurements were obtained with a Quantum Design magnetometer between 5 and 400 K in applied magnetic fields of up to 5 T.

The Mössbauer spectra have been measured between 4.2 and 295 K in a Janis Superveritemp cryostat on a constant-acceleration spectrometer which utilized a rhodium matrix cobalt-57 source and was calibrated at room temperature with  $\alpha$ -iron powder. The Mössbauer spectral absorbers contained approximately  $35 \text{ mg cm}^{-2}$  of powdered sample mixed with boron nitride. The Mössbauer spectra above 295 K have been measured in a vacuum, water-cooled, oven in which the temperature was controlled with a thermocouple with a relative accuracy of  $\pm 1\%$ . The Mössbauer absorber for the high temperature experiments consists of a thin pellet of  $\text{Mn}_{1.1}\text{Fe}_{0.9}\text{P}_{0.74}\text{Ge}_{0.26}$  mixed with boron nitride and pressed under  $1 \text{ g ton cm}^{-2}$ . The statistical errors on the refined Mössbauer spectral parameters are given in parentheses and the absolute errors are approximately twice as large.

## 3. Results

### 3.1. X-ray diffraction results

The room temperature powder x-ray diffraction patterns of the  $\text{Mn}_{1.1}\text{Fe}_{0.9}\text{P}_{1-x}\text{Ge}_x$  compounds, with  $x = 0.19, 0.22$  and  $0.25$ , are shown in figure 1. They can be indexed in the hexagonal  $\text{Fe}_2\text{P}$ -type structure with the  $P\bar{6}2m$  space group. In this structure, the Mn atoms occupy the 3g sites, the Fe atoms occupy the 3f sites [12] and the P and Ge atoms randomly occupy the 1b and 2c sites. There is no indication of any impurity phase in the x-ray diffraction patterns. An electron probe microanalysis of  $\text{Mn}_{1.1}\text{Fe}_{0.9}\text{P}_{0.78}\text{Ge}_{0.22}$  shows the presence of 4 vol% of  $\text{Mn}_2\text{O}_3$  and an actual composition of  $\text{Mn}_{1.095}\text{Fe}_{0.951}\text{P}_{0.77}\text{Ge}_{0.215}$ , which is very close to the nominal composition. In this paper, we will refer to the nominal compositions.

The compositional dependence of the room temperature lattice parameters, unit-cell volume and  $c/a$  ratio is shown in figure 2. The overall increase in  $a$  and decrease in  $c$  with increasing germanium content is similar to that observed [12] in the  $\text{MnFeP}_{0.59}\text{Si}_{0.41-x}\text{Ge}_x$  compounds. The

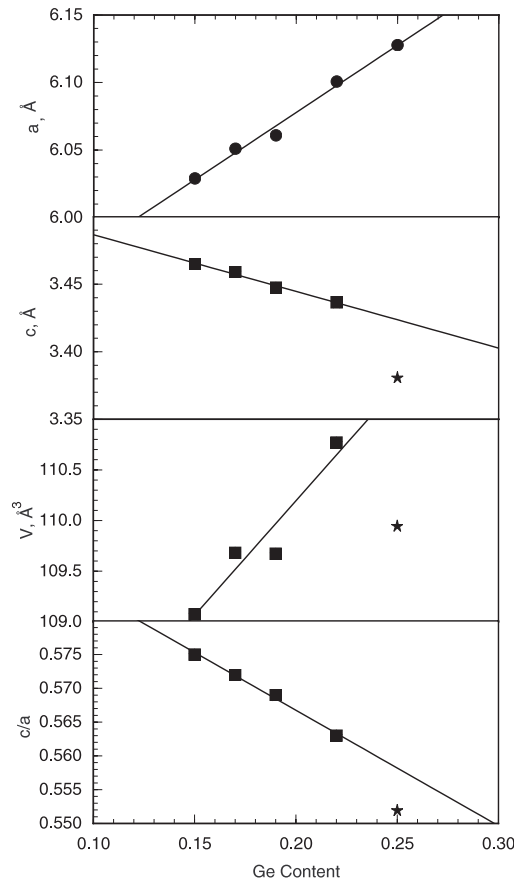


**Figure 2.** The compositional dependence of the lattice parameters, unit-cell volume and  $c/a$  ratio for the  $\text{Mn}_{1.1}\text{Fe}_{0.9}\text{P}_{1-x}\text{Ge}_x$  compounds. The data for  $x = 0.15$  and  $0.17$  are taken from [11]. The star indicates the composition  $x = 0.25$  that is ferromagnetic at room temperature.

lattice parameters, the unit-cell volume and the  $c/a$  ratio, given in table 1, show a linear compositional dependence from  $x = 0.15$  to  $0.22$ , as is clearly indicated by the solid lines in figure 2. The four compositions from  $x = 0.15$  to  $0.22$  are paramagnetic at room temperature, as is discussed in the next section, whereas  $\text{Mn}_{1.1}\text{Fe}_{0.9}\text{P}_{0.75}\text{Ge}_{0.25}$  is ferromagnetic at room temperature. Its smaller  $c$  lattice parameter, and hence unit-cell volume, and its smaller  $c/a$  ratio no doubt result from the magnetostriction present [11] at the Curie temperature. For  $\text{Mn}_{1.1}\text{Fe}_{0.9}\text{P}_{0.75}\text{Ge}_{0.25}$ , a  $\Delta V/V$  of 1.2% is obtained from the paramagnetic volume extrapolated from the straight line in figure 2 and the observed ferromagnetic volume. This is a large increase in volume in going from the ferromagnetic to the paramagnetic state, a large increase that contrasts with the small decrease of  $-0.07\%$  observed [11] in  $\text{Mn}_{1.1}\text{Fe}_{0.9}\text{P}_{0.85}\text{Ge}_{0.15}$ . Here it should be noted that a small decrease in volume observed when going from the ferromagnetic state to the paramagnetic state, or the corresponding increase in going from the paramagnetic state to the ferromagnetic state, is the normal behaviour for iron-based compounds due to the so-called invar effect [14].

In the course of this work, a preliminary report [15] of the temperature dependence of the unit-cell parameters of  $\text{Mn}_{1.1}\text{Fe}_{0.9}\text{P}_{0.8}\text{Ge}_{0.2}$  has become available. The 295 K lattice

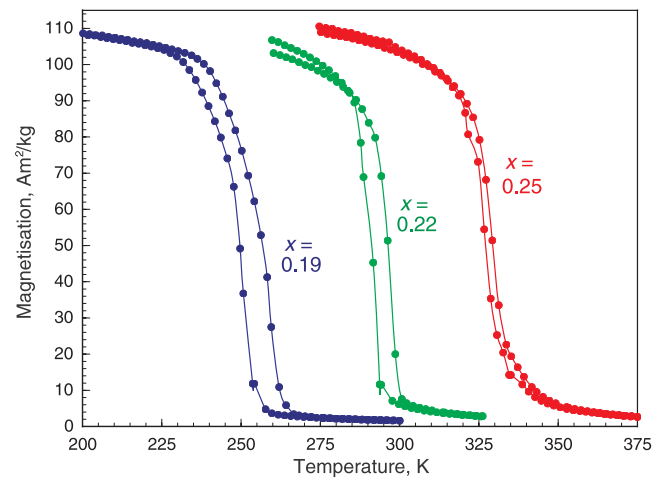


**Figure 3.** The temperature dependence of the magnetization in the  $\text{Mn}_{1.1}\text{Fe}_{0.9}\text{P}_{1-x}\text{Ge}_x$  compounds, with  $x = 0.19, 0.22$  and  $0.25$ .

**Table 1.** The  $\text{Mn}_{1.1}\text{Fe}_{0.9}\text{P}_{1-x}\text{Ge}_x$  lattice parameters, Curie temperatures, hysteresis widths and maximum change in isothermal magnetic entropy.

$x$	$a$ (Å)	$c$ (Å)	$V$ (Å <sup>3</sup> )	$c/a$	$T_C$ (K)	$\Delta T$ (K)	$-\Delta S_m$ (J kg <sup>-1</sup> K <sup>-1</sup> )
0.19	6.0609(5)	3.4474(5)	109.7	0.569	260	6	14
0.22	6.1007(5)	3.4366(5)	110.8	0.563	298	4	20
0.25	6.1277(5)	3.3812(5)	110.0	0.552	330	2	13

parameters are in reasonable agreement with the compositional dependence shown in figure 2, although the  $a$  and  $c$  lattice parameters are smaller and larger, respectively, than the linear extrapolated values and the unit cell is slightly larger. No significant change in unit-cell volume was observed at the ferromagnetic to paramagnetic transition, in contrast with the change postulated above from the compositional dependence at  $x = 0.25$ .

### 3.2. Magnetic measurements

The temperature dependence of the magnetization near the Curie temperature of the  $\text{Mn}_{1.1}\text{Fe}_{0.9}\text{P}_{1-x}\text{Ge}_x$  compounds, with  $x = 0.19, 0.22$  and  $0.25$ , is shown in figure 3. The Curie temperature increases with increasing germanium content, in agreement with the increase previously observed [11] for  $x = 0.15$  and  $0.17$ . The approximately 4 K width of the hysteresis is smaller than the 15 to 20 K width previously observed [11] for  $x = 0.15$  and  $0.17$  and is even smaller than the hysteresis width of 8 K observed [10] in the bulk alloy and melt spun ribbons of  $\text{Mn}_{1.1}\text{Fe}_{0.9}\text{P}_{0.76}\text{Ge}_{0.24}$ . The magnetic properties are summarized in table 1.

The maximum isothermal entropy change between zero and two tesla are given in table 1 and the temperature dependence of the isothermal magnetic entropy changes for field changes of 1 and 2 T are shown in figure 4. These changes and temperature dependences are similar to those observed for the other compositions [7, 10] of both the  $\text{Mn}_{1.1}\text{Fe}_{0.9}\text{P}_{1-x}\text{Ge}_x$  and  $\text{Mn}_{1.1}\text{Fe}_{0.9}\text{P}_{1-x}\text{As}_x$  compounds [4].

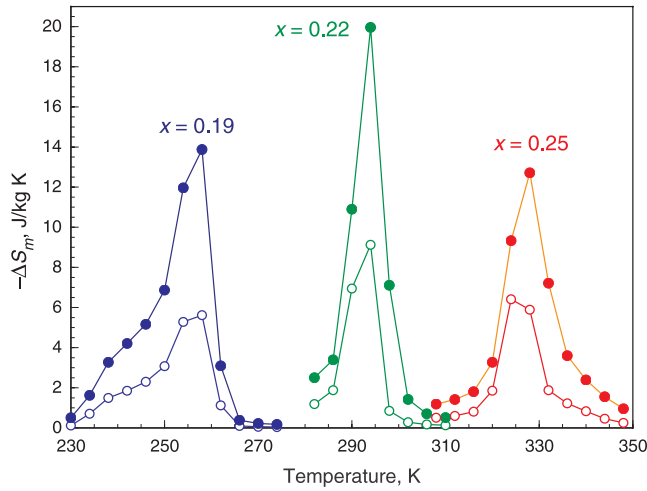


**Figure 4.** The isothermal magnetic entropy changes for a field change of 0–1 T, open symbols, and of 0–2 T, solid symbols.

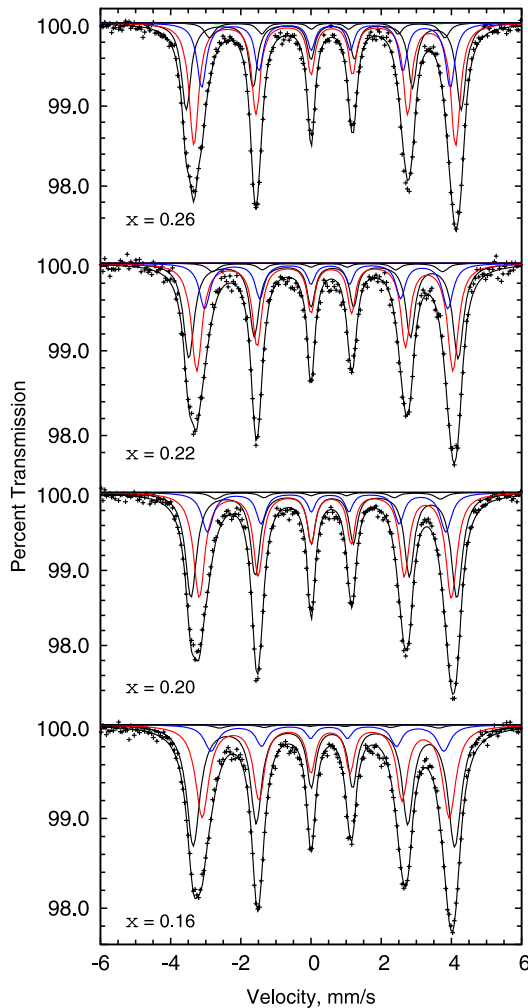


**Figure 5.** The 4.2 K Mössbauer spectra of the  $Mn_{1.1}Fe_{0.9}P_{1-x}Ge_x$  compounds, with  $x = 0.16, 0.20, 0.22$  and  $0.26$ .

The Curie temperature, magnetic hysteresis width and entropy changes reported [15] for  $Mn_{1.1}Fe_{0.9}P_{0.8}Ge_{0.2}$  are in reasonable agreement with the values given in table 1.

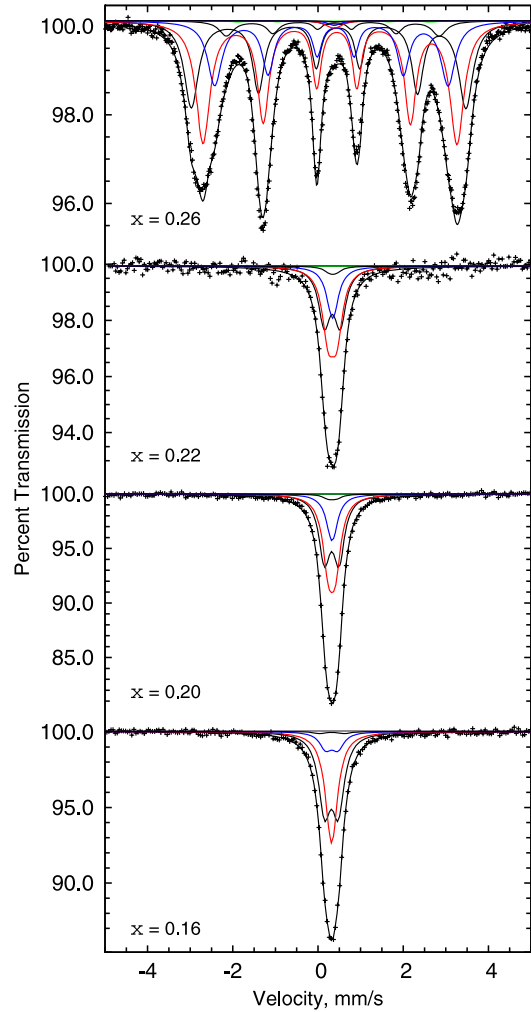


**Figure 6.** The 295 K Mössbauer spectra of the  $Mn_{1.1}Fe_{0.9}P_{1-x}Ge_x$  compounds, with  $x = 0.16, 0.20, 0.22$  and  $0.26$ .

### 3.3. Mössbauer spectral results

The Mössbauer spectra of the  $Mn_{1.1}Fe_{0.9}P_{1-x}Ge_x$  compounds, with  $x = 0.16, 0.20, 0.22$  and  $0.26$ , obtained at 4.2 K are shown in figure 5. All the spectra exhibit similar sextets that are associated with the ferromagnetic phase of a solid-solution compound, in which the distribution of phosphorus and germanium over the 1b and 2c sites gives rise to broad absorption lines as a result of the distribution of hyperfine fields,  $H$ , resulting from a different number of germanium near neighbours of the iron. All the ferromagnetic spectra were fitted with a binomial distribution model, as previously described [5] for the analysis of the Mössbauer spectra of the  $Mn_{1.1}Fe_{0.9}P_{1-x}As_x$  compounds. This distribution assumes a random distribution of phosphorus and germanium over the 1b and 2c sites, in disagreement with the preferential 2c site occupation exhibited by germanium as determined [15] from neutron diffraction. However, this slight preference would be very difficult to model in the fit of the Mössbauer spectra. The hyperfine field, isomer shift and quadrupole splitting for zero germanium near neighbours are  $H(0)$ ,  $\delta(0)$  and  $\Delta E_Q(0)$ . For each additional germanium near



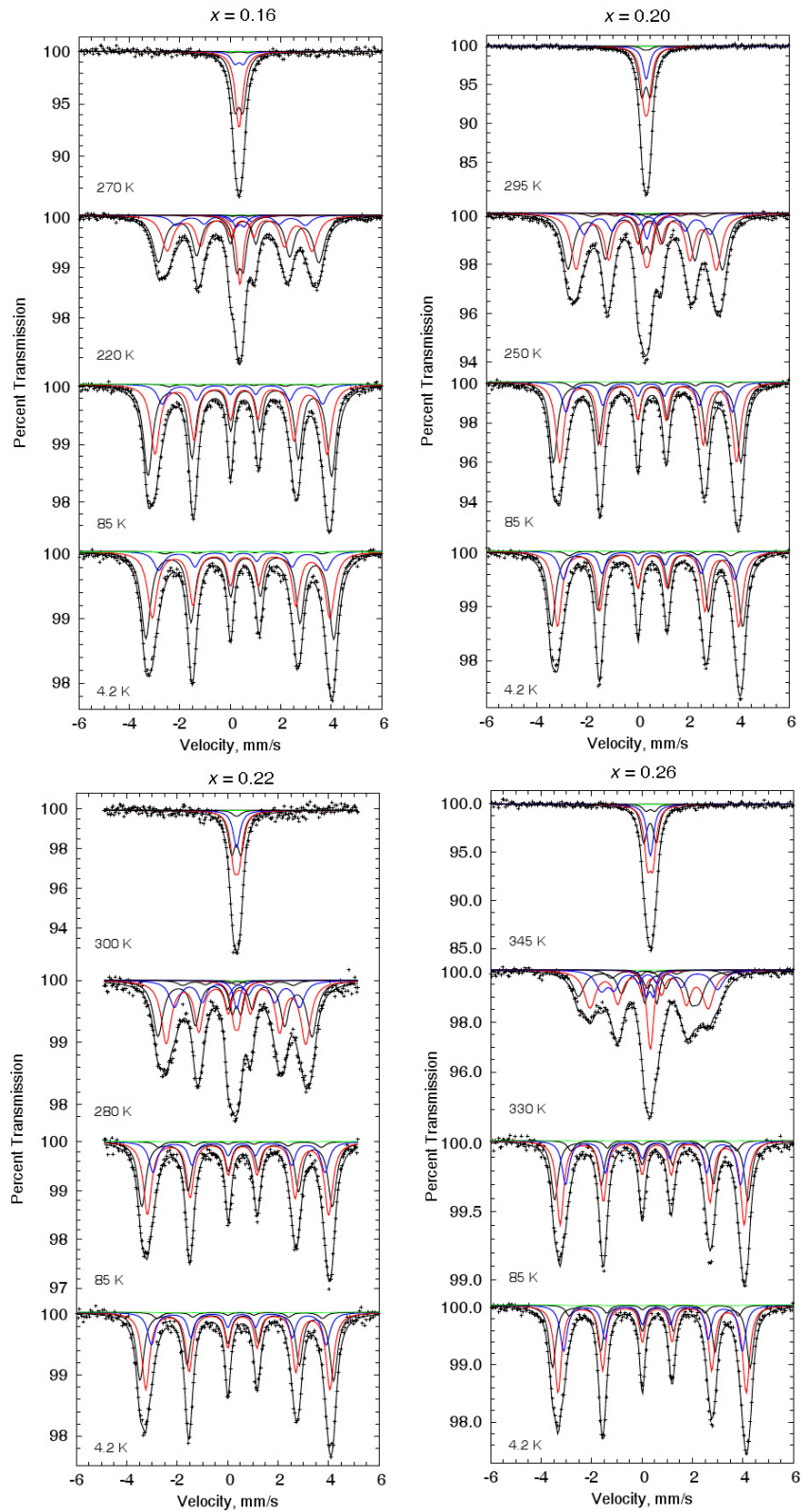


Figure 7. The Mössbauer spectra of  $\text{Mn}_{1.1}\text{Fe}_{0.9}\text{P}_{1-x}\text{Ge}_x$  obtained at the indicated temperatures.

neighbour, the hyperfine field,  $H$ , the isomer shift,  $\delta$ , and the quadrupole splitting,  $\Delta E_Q$ , was assumed to vary by an incremental hyperfine field,  $\Delta H$ , isomer shift,  $\Delta\delta$ , and quadrupole splitting,  $\Delta(\Delta E_Q)$ . For each composition,  $x$ , the

incremental isomer shift and the incremental quadrupole shift were first fitted as a function of temperature, and subsequently constrained to their thermal average—the preliminary fits indicated essentially temperature-independent values for these

parameters. Similarly, for each composition,  $x$ , the incremental isomer shift and the quadrupole splitting and its increment were first fitted for each paramagnetic subspectrum as a function of temperature, and subsequently constrained to their thermal average—the preliminary fits indicated essentially temperature-independent values for these parameters. Hence, in the final fits, the baseline, the spectral absorption area, the magnetic isomer shift,  $\delta(0)$ , the quadrupole shift,  $\varepsilon(0)$ , and the hyperfine field,  $H(0)$ , for zero germanium near neighbours, the percentage hyperfine field reduction,  $\Delta H$ , per additional germanium near neighbour, the paramagnetic isomer shift, the paramagnetic per cent area and one common linewidth were adjusted. The results of these fits are shown as the solid lines in figures 5–7. The different components resulting from the binomial distribution of germanium near neighbours are also shown in colour in figures 5–7. The resulting weighted average isomer shift,  $\langle\delta\rangle$ , quadrupole shift,  $\langle\varepsilon\rangle$ , hyperfine field,  $\langle H\rangle$ , the percentage hyperfine field reduction,  $\Delta H$ , the magnetic and paramagnetic linewidth,  $\Gamma$ , and the paramagnetic fraction,  $p$ , are given in table 2.

The Mössbauer spectra of the  $\text{Mn}_{1.1}\text{Fe}_{0.9}\text{P}_{1-x}\text{Ge}_x$  compounds, with  $x = 0.16, 0.20, 0.22$  and  $0.26$ , obtained at 295 K are shown in figure 6 and clearly reveal the variation in the Curie temperatures within the different compounds. The compositions with  $x = 0.16$ – $0.22$  are paramagnetic at 295 K whereas the composition  $x = 0.26$  is ferromagnetic.

Mössbauer spectra of  $\text{Mn}_{1.1}\text{Fe}_{0.9}\text{P}_{1-x}\text{Ge}_x$  at selected temperatures are shown in figure 7. The paramagnetic contribution to the spectra has been fitted with a binomial distribution of doublets in agreement with the distribution of germanium around the iron. The fit of the Mössbauer spectra showing the presence of both the ferromagnetic and paramagnetic phases was carried out with a binomial distribution associated with both the sextets and the doublets with the constraints described above for the paramagnetic subspectrum. The per cent area of the paramagnetic phase,  $p$ , has been fitted; a summary of the resulting hyperfine parameters is given in table 2.

#### 4. Discussion

Satisfactory fits of the Mössbauer spectra with the same isomer shift for the magnetic and paramagnetic subspectra could not be obtained. The good fits shown in figures 6 and 7 could only be obtained by using an isomer shift for the ferromagnetic phase larger than the isomer shift for the paramagnetic phase. This difference in isomer shift results from the magnetostriction observed at the ordering temperature. However, the smaller unit-cell volume observed for the ferromagnetic phase, see section 3.1, would be expected to lead [16] to a smaller isomer shift in contrast to observation. Hence, the unusual magnetostriction observed in the  $\text{Mn}_{1.1}\text{Fe}_{0.9}\text{P}_{1-x}\text{Ge}_x$  compounds results in a change in isomer shift at the ordering temperature that is not the unique consequence of the volume change. The decrease in isomer shift from the ferromagnetic to the paramagnetic phase must result from a combination of unit-cell volume increase and electronic structure changes.

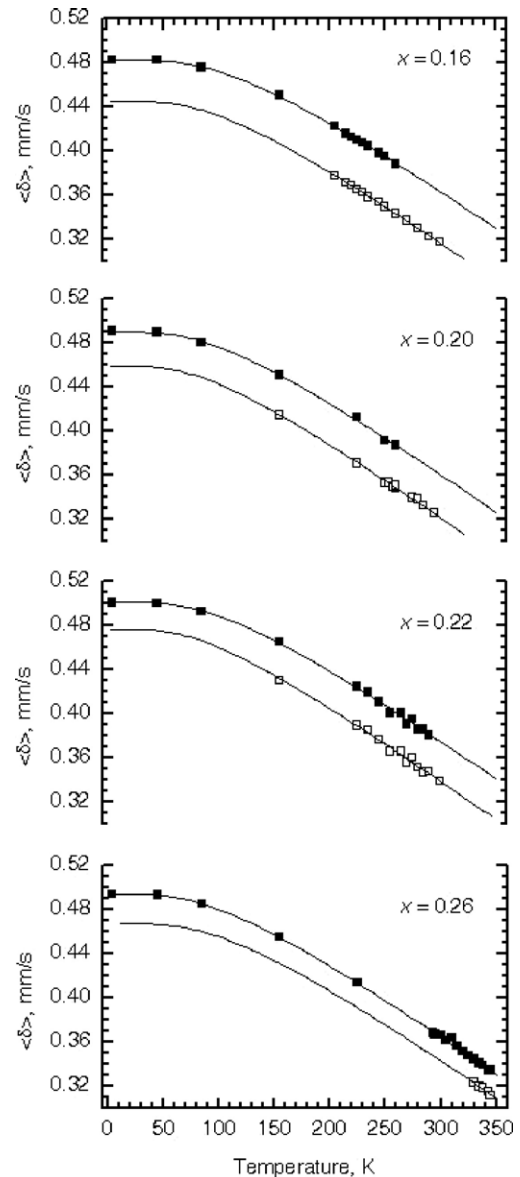


**Figure 8.** The temperature dependence of the weighted average isomer shift in the ferromagnetic (solid symbols) and paramagnetic (open symbols) phase of the  $\text{Mn}_{1.1}\text{Fe}_{0.9}\text{P}_{1-x}\text{Ge}_x$  compounds. The error bars are smaller than the data points. The solid lines are the result of a fit with the Debye model [17].

The temperature dependence of the weighted average isomer shifts in the ferromagnetic and paramagnetic phases of the  $\text{Mn}_{1.1}\text{Fe}_{0.9}\text{P}_{1-x}\text{Ge}_x$  compounds is shown in figure 8. The difference in isomer shift between the two phases is immediately obvious and exceeds the error bars of approximately  $0.002 \text{ mm s}^{-1}$  on the data points. This difference decreases from  $0.04$  to  $0.02 \text{ mm s}^{-1}$  between  $x = 0.16$  and  $0.26$ , respectively. The solid lines result from a fit with the Debye model [17] for the second-order Doppler shift. The Debye temperatures in the ferromagnetic and paramagnetic phases have been constrained to be equal and are  $452(6)$ ,  $395(10)$ ,  $412(20)$  and  $395(4)$  K for  $x = 0.16, 0.20, 0.22$  and  $0.26$ , respectively. These values are similar to the value of  $420(20)$  K observed [5] in the  $\text{MnFeP}_{1-x}\text{As}_x$  compounds. The

**Table 2.** Mössbauer spectral parameters for the  $\text{Mn}_{1.1}\text{Fe}_{0.9}\text{P}_{1-x}\text{Ge}_x$  compounds. (Note: the parameters are defined in the text and are given with statistical accuracies if they have been refined. The isomer shifts are given relative to room temperature  $\alpha$ -iron powder. The weighted average parameters obtained from the binomial fits are discussed in the text.)

$x$	$T$ (K)	Magnetic phase					Paramagnetic phase			Constraints ( $\text{mm s}^{-1}$ )	
		$\langle\delta\rangle$ ( $\text{mm s}^{-1}$ )	$\langle\varepsilon\rangle$ ( $\text{mm s}^{-1}$ )	$H(0)$ (T)	$\Delta H$ (%)	$\langle H\rangle$ (T)	$\Gamma$ ( $\text{mm s}^{-1}$ )	$\langle\delta\rangle$ ( $\text{mm s}^{-1}$ )	$\Gamma$ ( $\text{mm s}^{-1}$ )		$p$
0.26	345	—	—	—	—	—	0.319(2)	0.323(5)	1.000	$\Delta\delta = 0.003$	
	338	0.339	-0.117	16.1(5)	15	13.6(4)	0.359	0.325(2)	0.323(7)	0.81(1)	$\Delta\varepsilon = 0.06$
	330	0.345	-0.121(9)	17.03(7)	14.9(3)	14.4(4)	0.35(1)	0.331(4)	0.323	0.237(4)	$\Delta E_Q = -0.40$
	295	0.368(3)	-0.162(6)	20.48(6)	7.3(3)	18.9(9)	0.291(8)	0.4(1)	0.327	0.011(3)	$\Delta(\Delta E_Q) = 0.35$
	85	0.484(2)	-0.176(4)	23.81(4)	4.8(2)	22.6(9)	0.285(9)	—	—	0	
	4.2	0.493(2)	-0.199(3)	24.33(3)	4.8(1)	23.1(7)	0.264(6)	—	—	0	
0.22	300	—	—	—	—	—	0.338(3)	0.32(2)	1.000	$\Delta\delta = 0.004$	
	290	0.382	-0.11(2)	18.4(1)	11(1)	17(1)	0.41(4)	0.347(2)	0.328(2)	0.55(1)	$\Delta\varepsilon = 0.07$
	285	0.385(6)	-0.15(1)	18.63(8)	9.5(5)	17.1(9)	0.37(2)	0.347(4)	0.328	0.297(7)	$\Delta E_Q = -0.37$
	225	0.425(2)	-0.150(4)	21.47(3)	7.1(2)	20.1(5)	0.295(7)	0.390	0.328	0.035	$\Delta(\Delta E_Q) = 0.17$
	85	0.493(2)	-0.191(4)	23.45(4)	4.9(2)	22.4(9)	0.298(8)	—	—	0	
	4.2	0.499(2)	-0.192(4)	23.84(4)	4.9(2)	22.8(9)	0.276(8)	—	—	0	
0.20	295	—	—	—	—	—	0.325(1)	0.314(5)	1.000	$\Delta\delta = 0.004$	
	260	0.387(3)	-0.126(6)	18.33(4)	10.0(3)	16.9(5)	0.276(9)	0.348(1)	0.284(3)	0.479(4)	$\Delta\varepsilon = 0.07$
	250	0.391(3)	-0.135(5)	19.00(4)	9.2(3)	17.6(5)	0.330(8)	0.351	0.314	0.168(2)	$\Delta E_Q = -0.34$
	225	0.413(2)	-0.140(4)	20.31(3)	8.1(3)	19.0(4)	0.312(6)	0.372	0.314	0.060(2)	$\Delta(\Delta E_Q) = 0.18$
	85	0.480(2)	-0.163(3)	23.07(2)	5.6(2)	22.0(5)	0.278(6)	—	—	0	
	4.2	0.491(2)	-0.184(4)	23.53(3)	5.2(2)	22.56(7)	0.274(7)	—	—	0	
0.16	270	—	—	—	—	—	0.337(2)	0.34(2)	1.000	$\Delta\delta = 0.004$	
	260	0.386	-0.170	17.80	9.7	16.70	0.32	0.344(1)	0.308(6)	0.90(1)	$\Delta\varepsilon = 0.07$
	225	0.411(5)	-0.17(1)	19.77(6)	10(6)	18.4(7)	0.37(2)	0.365(3)	0.31(2)	0.317(7)	$\Delta E_Q = -0.32$
	205	0.425(3)	-0.138(5)	20.26(4)	8.3(4)	19.2(6)	0.306(8)	0.378	0.308	0.097	$\Delta(\Delta E_Q) = 0.31$
	85	0.477(2)	-0.157(5)	22.57(3)	6.4(2)	21.6(5)	0.343(7)	—	—	0	
	4.2	0.485(2)	-0.172(4)	23.16(3)	5.7(2)	22.3(6)	0.306(7)	—	—	0	

4.2 K weighted average isomer shift increases from  $x = 0.16$  to 0.22 in agreement with the increase in unit-cell volume.

The temperature dependence of both the weighted average hyperfine field and of the paramagnetic fraction,  $p$ , in the  $\text{Mn}_{1.1}\text{Fe}_{0.9}\text{P}_{1-x}\text{Ge}_x$  compounds is shown in figure 9. The coexistence [5] of the ferromagnetic and paramagnetic phases over relatively broad temperature ranges of up to 50 K is characteristic of samples exhibiting compositional inhomogeneities and hysteretic behaviour and has previously been observed [15] in  $\text{Mn}_{1.1}\text{Fe}_{0.9}\text{P}_{0.8}\text{Ge}_{0.2}$ . The increase in the paramagnetic fraction,  $p$ , with increasing temperature results from a distribution of the Curie temperature in different sample grains. The solid line in figure 9 is a fit with equation (6) in [5], a fit that assumes a Gaussian distribution of the Curie temperature in the different sample grains. This fit yields the Curie temperature,  $T_C$ , and the width of the distribution,  $w$ , given in table 3. The observed Curie temperatures are in good agreement with those obtained from magnetic measurements on slightly different compositions and given in table 1. The width of the distribution,  $w$ , is similar to the hysteresis width obtained from magnetization measurements and compares well with the hysteresis width observed on slightly different compositions, see table 1. The temperature dependences of the paramagnetic fraction in the present sample and the previously studied [15] sample of  $\text{Mn}_{1.1}\text{Fe}_{0.9}\text{P}_{0.8}\text{Ge}_{0.2}$  are very similar. The Curie temperature of 260.6 K and the hysteresis width of approximately 8 K obtained herein are slightly different from the 251 and 15 K previously reported. These small differences no doubt result from slight differences in the actual

**Table 3.** The  $\text{Mn}_{1.1}\text{Fe}_{0.9}\text{P}_{1-x}\text{Ge}_x$  Curie temperatures, hysteresis widths, zero Kelvin average magnetic hyperfine fields and order parameters.

$x$	$T_C$ (K)	$w$ (K)	$\langle H_0\rangle$ (T)	$\eta$
0.16	235.1(4)	14.4(5)	21.4(2)	2.34(7)
0.20	260.6(7)	7.8(5)	22.2(2)	1.72(5)
0.22	288.5(7)	5.9(3)	22.4(1)	1.69(3)
0.26	333.5(1)	3.4(5)	22.9(2)	1.33(4)

composition of samples with the same nominal composition and differences in the phosphorus and germanium distribution. The Mössbauer spectra are obtained over 24–48 h, i.e. a period of time long enough to ensure thermodynamic equilibrium between the paramagnetic and ferromagnetic phases of the material and hence the paramagnetic fraction plotted in figure 9 may be assumed to have reached thermodynamic equilibrium.

The Curie temperature and hysteresis width obtained from the Mössbauer spectra and the magnetic measurements are plotted as a function of germanium content in figure 10. The Curie temperature increases linearly with a slope of 1000 K per germanium atom. The hysteresis width decreases linearly with a slope of 100 K per germanium atom.

The 4.2 K weighted average hyperfine fields of approximately 23 T result from the relatively small magnetic moment measured on the 3f iron/manganese site. At 245 K in  $\text{Mn}_{1.1}\text{Fe}_{0.9}\text{P}_{0.8}\text{Ge}_{0.2}$  a moment of  $0.9 \mu_B$  was measured [15], whereas a field of 17.6 T is measured at 250 K for  $x = 0.20$ , see table 2. This gives a ratio of  $20 \text{ T}/\mu_B$ , a



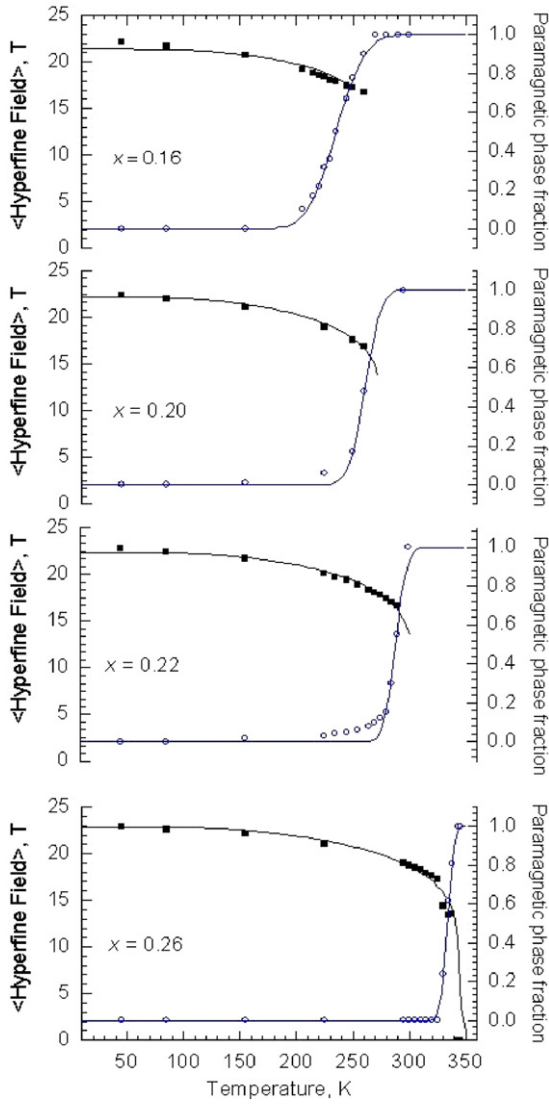


**Figure 9.** The temperature dependence of the weighted average hyperfine field (solid symbols) and the paramagnetic fraction,  $p$  (open symbols) for the  $\text{Mn}_{1.1}\text{Fe}_{0.9}\text{P}_{1-x}\text{Ge}_x$  compounds. The solid lines are the results of the fits described in the text.

value that is greater than the usually accepted value of  $15 \text{ T}/\mu_{\text{B}}$ . The  $4.2 \text{ K}$  weighted average hyperfine fields in the  $\text{Mn}_{1.1}\text{Fe}_{0.9}\text{P}_{1-x}\text{Ge}_x$  compounds are larger than those measured [5] in the  $\text{Mn}_{1.1}\text{Fe}_{0.9}\text{P}_{1-x}\text{As}_x$  compounds. This difference may result from the different orientation [15] of the magnetic moments in the two series of compounds.

The temperature dependence of the weighted average hyperfine field has been fitted with the Bean and Rodbell [18] magnetostriction exchange model with equation (7) in [5]<sup>5</sup>. The zero Kelvin hyperfine field and the transition-order parameter,  $\eta$ , resulting from the fit are given in table 3. All  $\eta$  values are larger than 1 and indicate that the ferromagnetic to paramagnetic transition is first order. The first-order character increases from  $x = 0.26$  to  $0.16$  in agreement with the concomitant increase in hysteresis width. It is

<sup>5</sup> It should be noted that a typographical error occurred in equation (7) in [5]. The denominator of the second term in the parenthesis is  $16(S + 1)^3 S$ .

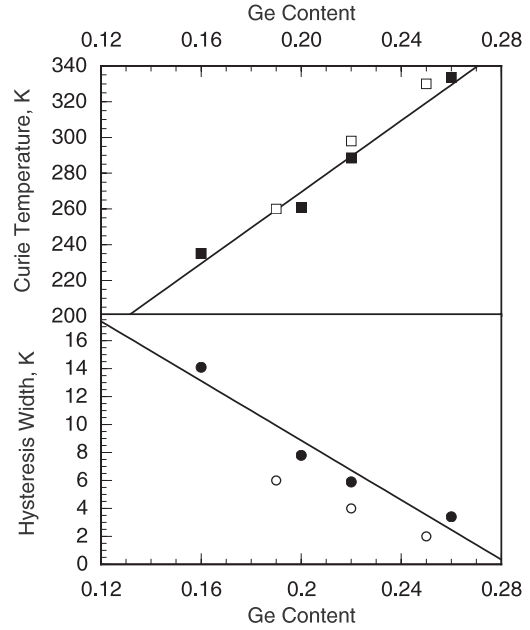


**Figure 10.** The compositional dependence of the Curie temperature and the hysteresis width in the  $\text{Mn}_{1.1}\text{Fe}_{0.9}\text{P}_{1-x}\text{Ge}_x$  compounds. The solid and open symbols indicate values obtained from the Mössbauer spectra and the magnetic measurements, respectively. The solid lines are the result of a least-squares fit of the values obtained from the Mössbauer spectra.

interesting to note that the difference in isomer shift between the ferromagnetic and the paramagnetic phase also increases with increasing  $\eta$  value. This correlation strongly supports the link between magnetostriction and isomer shift values.

In the Bean and Rodbell [18] magnetostriction exchange model, the transition-order parameter,  $\eta$ , is given by

$$\eta = (5/2)\{[4S(S + 1)]^2 / [(2S + 1)^4 - 1]\} NkKT_0\beta^2, \quad (1)$$

where  $N$  is the number of particles per unit volume,  $k$  is the Boltzmann constant,  $K$  is the compressibility,  $S = 2$  and  $\beta$  is the slope of the change in the transition temperature due to the magnetostriction and is defined by

$$T_C = T_0[1 + \beta(V - V_0)/V_0], \quad (2)$$

where  $T_C$  is the Curie temperature,  $T_0$  would be the Curie temperature in the absence of magnetostriction,  $V$  is the unit-cell volume and  $V_0$  would be the unit-cell volume in the absence of exchange interactions. For  $\text{Mn}_{1.1}\text{Fe}_{0.9}\text{P}_{0.74}\text{Ge}_{0.26}$ ,  $V$  is the observed unit-cell volume of  $109.95 \text{ \AA}^3$ , a  $V_0$  value of  $111.32 \text{ \AA}^3$  may be obtained from the extrapolation of the straight line in figure 2,  $T_C$  is  $333.5 \text{ K}$  and  $T_0$  is taken as the temperature at which a non-zero paramagnetic fraction appears, i.e.  $300 \text{ K}$ . Equation (2) then yields  $\beta$  equals  $-9.07$ . From the value of  $\eta$  of  $1.33$ , a compressibility  $K$  of  $2 \times 10^{-11} \text{ Pa}^{-1}$  is obtained from equation (1). This compressibility is approximately four times larger than the compressibility of  $4.8 \times 10^{-12} \text{ Pa}^{-1}$  measured [19] on  $\text{Fe}_2\text{P}$  and certainly accounts for the first-order transition in  $\text{Mn}_{1.1}\text{Fe}_{0.9}\text{P}_{0.74}\text{Ge}_{0.26}$ .

## 5. Conclusions

The Mössbauer spectra between 4.2 and 340 K of the  $\text{Mn}_{1.1}\text{Fe}_{0.9}\text{P}_{1-x}\text{Ge}_x$  compounds, with  $x = 0.16, 0.20, 0.22$  and  $0.26$ , have been successfully fitted with a distribution of hyperfine field and isomer shift in the ferromagnetic phase, a distribution of isomer shift and quadrupole splitting in the paramagnetic phase and a superposition of these two distributions in the magnetic transition region. These fits reveal a significant decrease in isomer shift from the ferromagnetic to the paramagnetic phase, a decrease that cannot be explained by the increase in unit-cell volume at the magnetic transition and indicates that significant electronic structure changes must occur at the magnetic transition.

The large and unusually negative magnetostriction in going from the paramagnetic to the ferromagnetic phase has been investigated through the temperature dependence of the average magnetic hyperfine field, a dependence that is well fitted by the Bean and Rodbell [18] model. From the order parameter,  $\eta$ , of the transition, the compressibility of  $\text{Mn}_{1.1}\text{Fe}_{0.9}\text{P}_{0.74}\text{Ge}_{0.26}$  is estimated to be in reasonable agreement with the observed [19] compressibility of  $\text{Fe}_2\text{P}$ .

In conclusion, both the Mössbauer isomer shift and hyperfine field are good indicators of the first-order transition in the  $\text{Mn}_{1.1}\text{Fe}_{0.9}\text{P}_{1-x}\text{Ge}_x$  compounds.

## Acknowledgments

This work was partially supported by the Fonds National de la Recherche Scientifique, Belgium, through grants 9.456595 and 1.5.064.05 and by the Dutch Technology Foundation (STW).

## References

- [1] Sales B C 2002 *Science* **295** 1248
- [2] Brück E 2005 *J. Phys. D: Appl. Phys.* **38** R381–91
- [3] Brück E, Tegus O, Cam Thanh D T, Trung N T and Buschow K H J 2008 *Intern. J. Refrig.* **31** 763
- [4] Tegus O, Brück E, Buschow K H J and de Boer F R 2002 *Nature* **415** 150
- [5] Hermann R P, Tegus O, Brück E, Buschow K H J, de Boer F R, Long G J and Grandjean F 2004 *Phys. Rev. B* **70** 214425
- [6] Brück E, Ilyin M and Tegus O 2005 *J. Magn. Magn. Mater.* **290** 8
- [7] Dagula W, Tegus O, Fuquan B, Zhang L, Si P Z, Zhang M, Shang W S, Brück E, de Boer F R and Buschow K H J 2005 *IEEE Trans. Magn.* **41** 2778
- [8] Dagula W, Tegus O, Li X W, Song L, Brück E, Cam Thanh D T, de Boer F R and Buschow K H J 2006 *J. Appl. Phys.* **99** 08Q105
- [9] Cam Thanh D T, Brück E, Tegus O, Klaasse J C P, Gortmulder T J and Buschow K H J 2006 *J. Appl. Phys.* **99** 08Q107
- [10] Yan A, Müller K-H, Schultz L and Gutfleisch O 2006 *J. Appl. Phys.* **99** 08K903
- [11] Yabuta H, Umeo K, Takabatake T, Koyama K and Watanabe K 2006 *J. Phys. Soc. Japan* **75** 113707
- [12] Cam Thanh D T, Brück E, Tegus O, Klaasse J C P and Buschow K H J 2007 *J. Magn. Magn. Mater.* **310** e1012
- [13] Yabuta H, Umeo K, Takabatake T, Chen L and Uwatoko Y 2007 *J. Magn. Magn. Mater.* **310** 1826
- [14] Shiga M 1994 Invar alloys *Materials Science and Technology* vol 3B, ed R W Cahn (Weinheim: VCH) pp 159–210
- [15] Liu D, Yue M, Zhang J, McQueen T M, Lynn J W, Wang X, Chen Y, Li J, Cava R J, Liu X, Altounian Z and Huang Q 2008 arXiv:0807.3707
- [16] Long G J, Pringle O A, Grandjean F and Buschow K H J 1992 *J. Appl. Phys.* **72** 4845
- [17] Shenoy G K, Wagner F E and Kalvius G M 1978 *Mössbauer Isomer Shifts* ed G K Shenoy and F E Wagner (Amsterdam: North-Holland) pp 49–110
- [18] Bean C P and Rodbell D S 1962 *Phys. Rev.* **126** 104
- [19] Fujii H, Hokabe T, Kamigaichi T and Okamoto T 1977 *J. Phys. Soc. Japan* **43** 41